A Class of Sparseness-controlled Algorithms for Echo Cancellation

Pradeep Loganathan, Andy W.H. Khong *Member, IEEE*, and
Patrick A. Naylor *Senior Member, IEEE*

***Abstract*—In the context of acoustic echo cancellation (AEC), it is shown that the level of sparseness in acoustic impulse responses can vary greatly in a mobile environment. When the response is strongly sparse, convergence of conventional approaches is poor. Drawing on techniques originally developed for network echo cancellation (NEC), we propose a class of AEC algorithms that can not only work well in both sparse and dispersive circumstances, but also adapt dynamically to the level of sparseness using a new sparseness-controlled approach. Simulation results, using white Gaussian noise (WGN) and speech input signals, show improved performance over existing methods. The proposed algorithms achieve these improvement with only a modest increase in computational complexity.**

Index Terms- Acoustic echo cancellation, Network echo cancellation, Sparse impulse responses, Adaptive algorithms

I. Introduction

ECHO cancellation in telephone networks comprising mixed packet-switched and circuit-switched components requires the identification and compensation of echo systems with various levels of sparseness. The network echo response in such systems is typically of length 64-128 ms, characterized by a bulk delay dependant on network loading, encoding and jitter buffer delays [1]. This results in an 'active' region in the range of 8-12 ms duration and consequently, the impulse response is dominated by 'inactive' regions where coefficient magnitudes are close to zero, making the impulse response sparse. The echo canceller must be robust to this sparseness [2]. This network echo cancellation (NEC) issue is particularly important in legacy networks comprising packet-switched and circuit switched components whereas in pure packet-switched networks NEC is not normally required.

Traditionally, adaptive filters have been deployed to achieve NEC by estimating the network echo response using algorithms such as the normalized least-mean-square (NLMS) algorithm.

Several approaches have been proposed over recent years to improve the performance of the standard NLMS algorithm in various ways for NEC. These include Fourier [3] and wavelet [4] based adaptive algorithms, variable step-size (VSS) algorithms [5], [6], [7], data reusing techniques [8], [9], partial update adaptive filtering techniques [10], [11] and sub-band adaptive filtering (SAF) schemes [12]. These approaches aim to address issues in echo cancellation including the performance with coloured input signals, time-varying echo paths and computational complexity, to name but a few. In contrast to these approaches, sparse adaptive algorithms have been developed specifically to address the performance of adaptive filters in sparse system identification. For sparse echo systems, the NLMS algorithm suffers from slow convergence [13].

Manuscript received –, 2008; revised –, 2008. The associate editor coordinating the review of this manuscript and approving it for publication was —.
The authors are with –. (e-mail: –). Digital Object Identifier –/LSP–

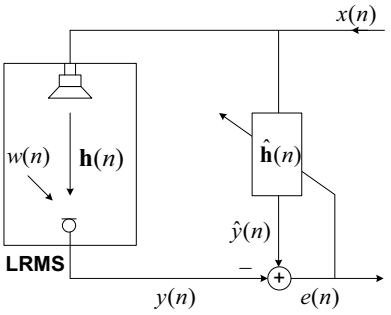

Fig. 1. Adaptive system for acoustic echo cancellation in a Loudspeaker-Room-Microphone system (LRMS).

One of the first sparse adaptive filtering algorithms for NEC is proportionate NLMS (PNLMS) [2] in which each filter coefficient is updated with an independent step-size that is linearly proportional to the magnitude of that estimated filter coefficient. It is well known that PNLMS has very fast initial convergence for sparse impulse responses after which its convergence rate reduces significantly, sometimes resulting in a slower overall convergence than NLMS. In addition, PNLMS suffers from slow convergence when estimating dispersive impulse responses [13], [14]. To address the latter problem, subsequent improved versions, such as PNLMS++ [14], were proposed. The PNLMS++ algorithm achieves improved convergence by alternating between NLMS and PNLMS for each sample period. However, as shown in [15], the PNLMS++ algorithm only performs best in the cases when the impulse response is sparse or highly dispersive.

An improved PNLMS (IPNLMS) [15] algorithm was proposed to exploit the 'proportionate' idea by introducing a controlled mixture of proportionate (PNLMS) and non-proportionate (NLMS) adaptation. A sparseness-controlled IPNLMS algorithm was proposed in [16] to improve the robustness of IPNLMS to the sparseness variation in impulse responses. Composite PNLMS and NLMS (CPNLMS) [17] adaptation was proposed to control the switching of PNLMS++ between the NLMS and PNLMS algorithms. For sparse impulse responses, CPNLMS performs the PNLMS adaptation to update the large coefficients and subsequently

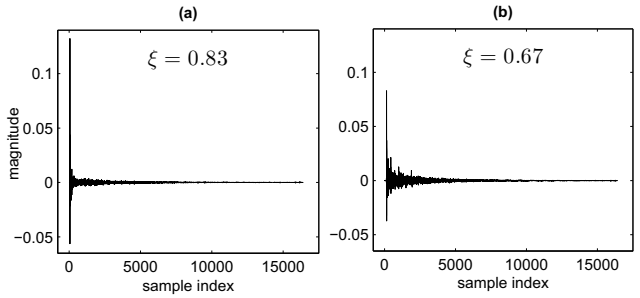

Fig. 2. Room impulse responses obtained, at 20 kHz sampling frequency, when the distances between a loudspeaker and a microphone are a) 75 cm and b) 185 cm, with room dimensions $3 \times 5 \times 3.5$ m. ξ represents the sparseness measure defined in Section III-A.

switches to NLMS, which has better performance for the adaptation of the remaining small taps. The μ-law PNLMS (MPNLMS) [18] algorithm was proposed to address the uneven convergence rate of PNLMS during the estimation process. As proposed in [18], MPNLMS uses optimal step-size control factors to achieve faster overall convergence until the adaptive filter reaches its steady state.

With the development of hands-free mobile telephony in recent years, another type of echo, acoustic echo, seriously degrades user experience due to the coupling between the loudspeaker and microphone. For this reason, effective acoustic echo cancellation (AEC) [19] is important to maintain usability and to improve the perceived voice quality of a call. Although sparse adaptive filtering algorithms, such as those described above, have originally been developed for NEC, it has been shown in [20] that such algorithms give good convergence performance in the AEC system as illustrated in Fig. 1.

The time variation of the near-end acoustic impulse response (AIR) may arise due to, for example, a change in temperature [21], pressure and changes in the acoustic environment. It is also well known that the reverberation time of an AIR is proportional to the volume of the enclosed space and inversely proportional to the absorption area [22]. For an outdoor environment, the reverberation time is reduced significantly due to the lack of reflections from any enclosure. The outdoor environment refers here to a typical urban area or a rural area with sparsely placed acoustically reflecting objects. The sparseness of the AIR of an outdoor environment is significantly greater than typical indoor environments and equally, if not more, variable.

Variation in the sparseness of AIRs can also occur in AEC within an enclosed space. Consider an example case where the distance, a, between a loudspeaker and the user using, for example, a wireless microphone is varying. Figure 2 shows two AIRs obtained in the same room, at 20 kHz sampling frequency, when a) $a = 75$ cm and b) $a = 185$ cm, with room dimensions $3 \times 5 \times 3.5$ m. As can be seen, the sparseness of these AIRs varies with the loudspeaker-microphone distance. Hence, algorithms developed for mobile hands-free terminals are required to be robust to the variations in the sparseness of the acoustic path.

In this paper, we propose a class of algorithms that are robust to the sparseness variation of AIRs. These algorithms compute a sparseness measure of the estimated impulse response at each iteration of the adaptive process and incorporate it into their conventional methods. As will be shown, the proposed sparseness-controlled algorithms achieve fast convergence for both sparse and dispersive AIRs and are effective for AEC.

II. Review of algorithms for echo cancellation

Figure 1 shows a Loudspeaker-Room-Microphone system (LRMS) and an adaptive filter $\widehat{\mathbf{h}}(n) = [\widehat{h}_0(n)\widehat{h}_1(n)\dots\widehat{h}_{L-1}(n)]^T$ deployed to cancel acoustic echo, where L is the length of the adaptive filter assumed to be equal to the unknown room impulse response and $[\cdot]^T$ is the transposition operator. Defining the input signal $\mathbf{x}(n) = [x(n)\ x(n-1)\ \dots\ x(n-L+1)]^T$ and $\mathbf{h}(n) = [h_0(n)\ h_1(n)\ \dots\ h_{L-1}(n)]^T$ as the unknown impulse response, the output of the LRMS is given by

$$y(n) = \mathbf{h}^T(n)\mathbf{x}(n) + w(n), \tag{1}$$

where $w(n)$ is additive noise and the error signal is given by

$$e(n) = y(n) - \widehat{\mathbf{h}}^T(n-1)\mathbf{x}(n). \tag{2}$$

Several adaptive algorithms such as those described below have been developed for either AEC or NEC.

Many adaptive algorithms can be described by (2) and the following set of equations:

$$\widehat{\mathbf{h}}(n) = \widehat{\mathbf{h}}(n-1) + \frac{\mu\mathbf{Q}(n-1)\mathbf{x}(n)e(n)}{\mathbf{x}^T(n)\mathbf{Q}(n-1)\mathbf{x}(n) + \delta}, \tag{3}$$

$$\mathbf{Q}(n-1) = \mathrm{diag}\{q_0(n-1)\ \dots\ q_{L-1}(n-1)\}, \tag{4}$$

where μ is a step-size and δ is the regularization parameter. The diagonal step-size control matrix $\mathbf{Q}(n)$ is introduced here to determine the step-size of each filter coefficient and is dependent on the specific algorithm.

A. The NLMS, PNLMS and MPNLMS algorithms

The NLMS algorithm is one of the most popular for AEC due to its straightforward implementation and low complexity compared to, for example, the recursive least squares algorithm. For NLMS, since the step-size is the same for all filter coefficients, $\mathbf{Q}(n) = \mathbf{I}_{L\times L}$ with $\mathbf{I}_{L\times L}$ being an $L \times L$ identity matrix.

One of the main drawbacks of the NLMS algorithm is that its convergence rate reduces significantly when the impulse response is sparse, such as often occurs in NEC. The poor performance has been addressed by several sparse adaptive algorithms such as those described below that have been developed specifically to identify sparse impulse responses in NEC applications.

The PNLMS and MPNLMS algorithms have been proposed for sparse system identification. Diagonal elements q_l of the step-size control matrix $\mathbf{Q}(n)$ for the PNLMS [2] and

MPNLMS [18] algorithms can be expressed as

$$q_l(n)=\frac{\kappa_l(n)}{\frac{1}{L}\sum_{i=0}^{L-1}\kappa_i(n)}, \qquad 0\le l\le L-1, \tag{5}$$

$$\kappa_l(n)=\max\Big\{\rho\times\max\{\gamma, F(|\widehat{h}_0(n)|)\ \ldots\ F(|\widehat{h}_{L-1}(n)|)\}, F(|\widehat{h}_l(n)|)\Big\}, \tag{6}$$

where $F(|\widehat{h}_l(n)|)$ is specific to the algorithm. The parameter $\gamma = 0.01$ in (6) prevents the filter coefficients $\widehat{h}_l(n)$ from stalling when $\widehat{\mathbf{h}}(0) = \mathbf{0}_{L\times 1}$ at initialization and ρ, with a typical value of 0.01, prevents the coefficients from stalling when they are much smaller than the largest coefficient.

The PNLMS algorithm achieves a high rate of convergence by employing step-sizes that are proportional to the magnitude of the estimated impulse response coefficients where elements $F(|\widehat{h}_l(n)|)$ are given by

$$F(|\widehat{h}_l(n)|) = |\widehat{h}_l(n)|. \tag{7}$$

Hence, PNLMS employs larger step-sizes for 'active' coefficients than for 'inactive' coefficients and consequently achieves faster convergence than NLMS for sparse impulse responses. However, it is found that PNLMS achieves fast initial convergence followed by a slower second phase convergence [18].

The MPNLMS algorithm was proposed to improve the convergence of PNLMS. It achieves this by computing the optimal proportionate step-size during the adaptation process. The MPNLMS algorithm was derived such that all coefficients attain a converged value to within a vicinity ϵ of their optimal value in the same number of iterations [18]. As a consequence, $F(|\widehat{h}_l(n)|)$ for MPNLMS is specified by

$$F(|\widehat{h}_l(n)|) = \ln(1+\beta|\widehat{h}_l(n)|), \tag{8}$$

with $\beta = 1/\epsilon$ and ϵ is a very small positive number chosen as a function of the noise level [18]. It has been shown that $\epsilon = 0.001$ is a good choice for typical echo cancellation. The positive bias of 1 in (8) is introduced to avoid numerical instability during the initialization stage when $|\widehat{h}_l(0)| = 0, \forall l$.

It is important to note that both PNLMS and MPNLMS suffer from slow convergence when the unknown system $\mathbf{h}(n)$ is dispersive [14], [13]. This is because when $\mathbf{h}(n)$ is dispersive, $\kappa_l(n)$ in (6) becomes significantly large for most $0 \le l \le L-1$. As a consequence, the denominator of $q_l(n)$ in (5) is large, giving rise to a small step-size for each large coefficient. This causes a significant degradation in convergence performance for PNLMS and MPNLMS when the impulse response is dispersive such as can occur in AIRs.

B. The IPNLMS algorithm

The IPNLMS [15] algorithm was originally developed for NEC and was further developed for the identification of acoustic room impulse responses [20]. It employs a combination of proportionate (PNLMS) and non-proportionate (NLMS) adaptation, with the relative significance of each controlled by a factor α_{IP} such that the diagonal elements of $\mathbf{Q}(n)$ are given as

$$q_l(n) = \frac{1-\alpha_{\mathrm{IP}}}{2L}+\frac{(1+\alpha_{\mathrm{IP}})|\widehat{h}_l(n)|}{2\|\widehat{\mathbf{h}}(n)\|_1+\delta_{\mathrm{IP}}}, \qquad 0\le l\le L-1. \tag{9}$$

where $\|\cdot\|_1$ is defined as the l_1-norm and the first and second terms are the NLMS and the proportionate terms respectively. It can be seen that IPNLMS is the same as NLMS when $\alpha_{\mathrm{IP}} = -1$ and PNLMS when $\alpha_{\mathrm{IP}} = 1$. Use of a higher weighting for NLMS adaptation, such as α_{IP} = 0, -0.5 or -0.75, is a favorable choice for most AEC/NEC applications [15]. It has been shown that, although the IPNLMS algorithm has faster convergence than NLMS and PNLMS regardless of the impulse response nature [15], we note from our simulations that it does not outperform MPNLMS for highly sparse impulse responses with the above choices of α_{IP}.

III. Characterization of framework for robust convergence

In this Section, we quantify the degree of sparseness in AIRs. We provide an illustrative example to show how the sparseness of AIRs varies with the loudspeaker-microphone distance in an enclosed space such as when the user is using a wireless microphone for tele/video conferencing. This serves as a motivation for us to develop new algorithms which are robust to the sparseness variation of AIRs in the next Section. In addition, we also demonstrate how the choice of ρ in (6) affects the step-size of each filter coefficient for PNLMS.

A. Variation of sparseness in AIRs

The degree of sparseness for an impulse response can be quantified by [16], [23]

$$\xi(n) = \frac{L}{L-\sqrt{L}}\left\{1-\frac{\|\mathbf{h}(n)\|_1}{\sqrt{L}\ \|\mathbf{h}(n)\|_2}\right\} \tag{10}$$

It can be shown [16], [23] that $0 \le \xi(n) \le 1$. In the extreme but unlikely case when

$$h_l(n) = \begin{cases} \pm k, & l = l_1, \\ 0, & 0\le l\le L-1,\ l\ne l_1, \end{cases} \tag{11}$$

where $l_1 \in \{[0, L-1]\}$ and $k \in \Re$, then $\xi(n) = 1$. On the other hand, when $h_l(n) = \pm k\ \forall l$, then $\xi(n) = 0$. In reality $\mathbf{h}(n)$ and hence $\xi(n)$ is time-varying and depends on factors such as temperature, pressure and reflectivity [21]. As explained in Section I, the sparseness of AIRs $\xi(n)$ varies with the location of the receiving device in an open or enclosed environment. We show below how $\xi(n)$ can also vary with the loudspeaker-microphone distance in an enclosed space.

Consider an example case where the distance, a, between a fixed position loudspeaker and the talker using a wireless microphone is varying. Figure 3 shows two AIRs, generated using the method of images [24], [25] with 1024 coefficients using room dimensions of $8\times10\times3$ m and 0.57 as the reflection coefficient. The loudspeaker is fixed at $4\times9.1\times1.6$ m in the LRMS while the microphone is positioned at $4\times8.2\times1.6$ m and $4\times1.4\times1.6$ m giving impulse responses as shown in Fig. 3

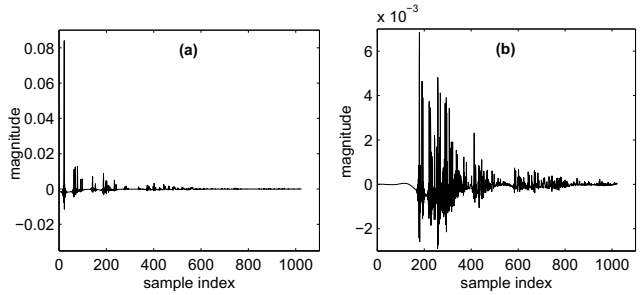

Fig. 3. Acoustic impulse responses

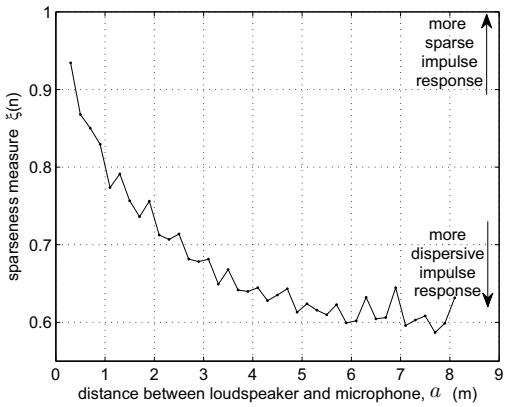

Fig. 4. Sparseness measure against the distance between loudspeaker and microphone, a. The impulse responses are obtained from the image model using a fixed room dimensions of $8 \times 10 \times 3$ m.

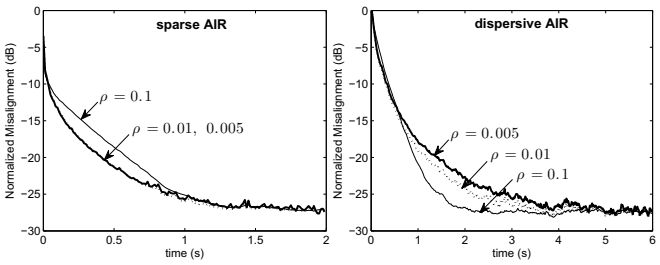

Fig. 5. Convergence of the PNLMS for different values of ρ using WGN input signal. Impulse responses in Fig. 3 (a) and (b) are used as sparse and dispersive AIRs respectively. [$\mu_{\mathrm{PNLMS}} = 0.3$, SNR $= 20$ dB]

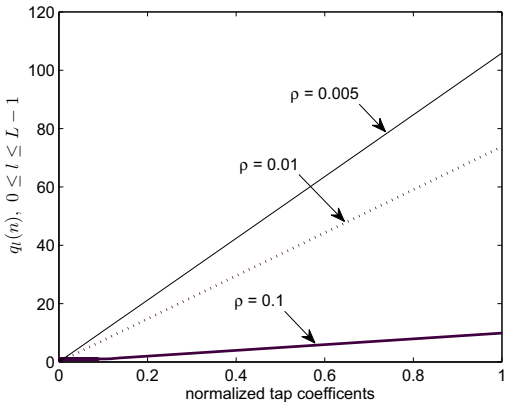

Fig. 6. Magnitude of $q_l(n)$ for $0 \leq l \leq L-1$ against the magnitude of coefficients $\widehat{h}_l(n)$ in PNLMS.

(a) and (b) for $a = 0.9$ m and $a = 7.7$ m respectively. Figure 4 illustrates how $\xi(n)$ of such AIRs varies with a. For each loudspeaker-microphone distance a, the microphone is directly in front of the loudspeaker. As can be seen, $\xi(n)$ reduces with increasing a, since for increasing a, the sound field becomes more diffuse. Since $\xi(n)$ varies with a, we propose to incorporate $\xi(n)$ into PNLMS, MPNLMS and IPNLMS in order to improve their robustness to the sparseness of AIRs in AEC. Since $\mathbf{h}(n)$ is unknown during adaptation, we employ $\widehat{\xi}(n)$ to estimate the sparseness of an impulse response, where at each sample iteration,

$$\widehat{\xi}(n) = \frac{L}{L-\sqrt{L}}\left\{1 - \frac{\|\widehat{\mathbf{h}}(n)\|_1}{\sqrt{L}\ \|\widehat{\mathbf{h}}(n)\|_2}\right\}. \qquad (12)$$

B. Effect of ρ on step-size control matrix $\mathbf{Q}(n)$ for PNLMS

As explained in Section II-A, the parameter ρ in (6) was originally introduced to prevent freezing of the filter coefficients when they are much smaller than the largest coefficient. Figure 5 shows the effect of ρ for both sparse and dispersive AIRs on the convergence performance of PNLMS measured using the normalized misalignment defined by

$$\eta(n) \ = \ \frac{\|\mathbf{h}(n) - \widehat{\mathbf{h}}(n)\|_2^2}{\|\mathbf{h}(n)\|_2^2}. \qquad (13)$$

A zero mean white Gaussian noise (WGN) sequence is used as the input signal while another WGN sequence $w(n)$ is added to give an SNR of 20 dB. Impulse responses as shown in Fig. 3 (a) and (b) are used as sparse and dispersive AIRs, and $\mu_{\mathrm{PNLMS}} = 0.3$. It can be seen from this illustration that, for a sparse $\mathbf{h}(n)$, we desire a low value of ρ while, for a dispersive unknown system $\mathbf{h}(n)$, we desire a high value of ρ. This is due to the resulting effect of how different values of ρ affect the step-size control element $q_l(n)$ as illustrated in Fig. 6. It can be observed that a higher value of ρ will reduce the influence of the proportional update term meaning that all filter coefficients are updated at a more uniform rate. This provides a good convergence performance for PNLMS for a dispersive AIR. On the other hand, a lower ρ will increase the degree of proportionality hence giving good convergence performance when the AIR is sparse. As a consequence of this important observation, we propose to incorporate $\widehat{\xi}(n)$ into ρ for both PNLMS and MPNLMS as described in the next section.

IV. A CLASS OF SPARSENESS-CONTROLLED ALGORITHMS

We propose to improve the robustness of PNLMS, MPNLMS and IPNLMS to varying levels of sparseness of impulse response such as encountered in, for example, AEC. As will be shown in the following, this is achieved by incorporating the sparseness measure of the estimated AIRs into the adaptation process. We will discuss these approaches conceptually and with simulation results on both WGN and speech. For an analytical prospective, the reader is referred to [26].

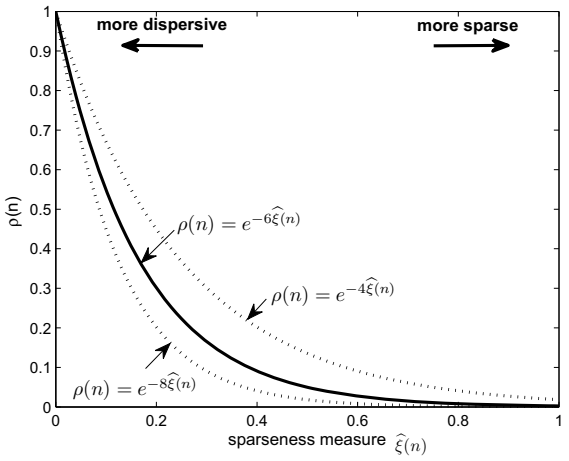

Fig. 7. Variation of ρ against sparseness measure $\widehat{\xi}(n)$ of impulse response.

A. The proposed SC-PNLMS and SC-MPNLMS algorithms

In order to address the problem of slow convergence in PNLMS and MPNLMS for dispersive AIR, we require the step-size control elements $q_l(n)$ to be robust to the sparseness of the impulse response. Several choices can be employed to obtain the desired effect of achieving a high ρ when $\widehat{\xi}(n)$ is small when estimating dispersive AIRs. We consider an example function

$$\rho(n) = e^{-\lambda\widehat{\xi}(n)}, \qquad \lambda \in \mathbb{R}^+. \tag{14}$$

The variation of $\rho(n)$ in PNLMS for the exponential function is plotted in Fig. 7 for the cases where $\lambda = 4, 6$ and 8. It can be noted that a linear function $\rho(n) = 1 - \widehat{\xi}(n)$ also achieves our desired condition. We have tested this case and found it to perform worse than the more general form of (14), so we will not consider it further.

It can be seen that low values of $\rho(n)$ are allocated for a large range of sparse impulse responses such as when $\widehat{\xi}(n) > 0.4$. As a result of small values in $\rho(n)$ using (14), the proposed sparseness-controlled PNLMS algorithm (SC-PNLMS) inherits the proportionality step-size control over a large range of sparse impulse response. When the impulse response is dispersive, such as when $\widehat{\xi}(n) < 0.4$, the proposed SC-PNLMS algorithm inherits the NLMS adaptation control with larger values of $\rho(n)$. As explained in Section III-B and Fig. 6, this gives a more uniform step-size across $h_l(n)$. Hence, the exponential function described by (14) will achieve our overall desired effect of the robustness to sparse and dispersive AIRs.

The choice of λ is important. As can be seen from Fig. 7, a larger choice of λ will cause the proposed SC-PNLMS to inherit more of PNLMS properties compared to NLMS giving good convergence performance when AIR is sparse. On the other hand, when the AIR is dispersive, λ must be small for good convergence performance. Hence, we show in Section VI-A that a good compromise is given by $\lambda = 6$, though the algorithm is not very sensitive to this choice in the range of $4 \leq \lambda \leq 6$.

Incorporating $\rho(n)$ in a similar manner for the MPNLMS algorithm, the resulting sparseness-controlled MPNLMS algorithm (SC-MPNLMS) inherits more of the MPNLMS properties when the estimated AIR is sparse and distributes uniform step-size across $h_l(n)$, as in NLMS, when the estimated AIR is dispersive. In addition, we note that when $n = 0$, $\|\widehat{\mathbf{h}}(0)\|_2 = 0$ and hence, to prevent division by a small number or zero, $\widehat{\xi}(n)$ can be computed for $n \geq L$ in both SC-PNLMS and SC-MPNLMS. When $n < L$, we set $\rho(n) = 5/L$ as described in [15]. The SC-PNLMS algorithm is thus described by (2)-(7), (12) and (14), whereas SC-MPNLMS is described by (2)-(6), (8), (12) and (14) with $\lambda = 6$, as summarized in Table I.

TABLE I
THE SPARSENESS-CONTROLLED ALGORITHMS

Initialisations:

$$\begin{aligned}
&\widehat{\mathbf{h}}(0) = \mathbf{0}_{L\times 1}\\
&0 < \mu \leq 1\\
&\alpha_{\mathrm{SC-IP}} = -0.75 && \text{(SC-IPNLMS)}\\
&\lambda = 6 && \text{(SC-PNLMS, SC-MPNLMS)}\\
&\rho(n) = 5/L, \quad n < L && \text{(SC-PNLMS, SC-MPNLMS)}\\
&\beta = 1000 && \text{(SC-MPNLMS)}
\end{aligned}$$

General Computations:

$$\begin{aligned}
e(n) &= y(n) - \widehat{\mathbf{h}}^T(n-1)\mathbf{x}(n)\\
\widehat{\mathbf{h}}(n) &= \widehat{\mathbf{h}}(n-1) + \frac{\mu\mathbf{Q}(n-1)\mathbf{x}(n)e(n)}{\mathbf{x}^T(n)\mathbf{Q}(n-1)\mathbf{x}(n) + \delta}\\
\mathbf{Q}(n-1) &= \mathrm{diag}\{q_0(n-1), \ldots, q_{L-1}(n-1)\}\\
\widehat{\xi}(n) &= \frac{L}{L-\sqrt{L}}\left\{1 - \frac{\|\widehat{\mathbf{h}}(n)\|_1}{\sqrt{L}\,\|\widehat{\mathbf{h}}(n)\|_2}\right\}, \qquad n \geq L
\end{aligned}$$

SC-PNLMS

$$\begin{aligned}
q_l(n) &= \frac{\kappa_l(n)}{\frac{1}{L}\sum_{i=0}^{L-1}\kappa_i(n)}, \qquad 0 \leq l \leq L-1\\
\kappa_l(n) &= \max\Big\{\rho(n) \times \max\{\gamma,\\
&\qquad |\widehat{h}_0(n)|, \ldots, |\widehat{h}_{L-1}(n)|\}, |\widehat{h}_l(n)|\Big\}\\
\rho(n) &= e^{-\lambda\widehat{\xi}(n)}, \qquad n \geq L
\end{aligned}$$

SC-MPNLMS

$$\begin{aligned}
q_l(n) &= \frac{\kappa_l(n)}{\frac{1}{L}\sum_{i=0}^{L-1}\kappa_i(n)}, \qquad 0 \leq l \leq L-1\\
\kappa_l(n) &= \max\Big\{\rho(n) \times \max\{\gamma,\\
&\qquad \mathrm{F}(|\widehat{h}_0(n)|), \ldots, \mathrm{F}(|\widehat{h}_{L-1}(n)|)\}, \mathrm{F}(|\widehat{h}_l(n)|)\Big\}\\
\mathrm{F}(|\widehat{h}_l(n)|) &= \ln(1 + \beta|\widehat{h}_l(n)|)\\
\rho(n) &= e^{-\lambda\widehat{\xi}(n)}, \qquad n \geq L
\end{aligned}$$

SC-IPNLMS

$$\begin{aligned}
q_l(n) &= \Big[\frac{1 - 0.5\widehat{\xi}(n)}{L}\Big]\frac{(1-\alpha_{\mathrm{SC-IP}})}{2L} +\\
&\qquad \Big[\frac{1 + 0.5\widehat{\xi}(n)}{L}\Big]\frac{(1+\alpha_{\mathrm{SC-IP}})|\widehat{h}_l(n)|}{2\|\widehat{\mathbf{h}}(n)\|_1 + \delta_{\mathrm{IP}}}
\end{aligned}$$

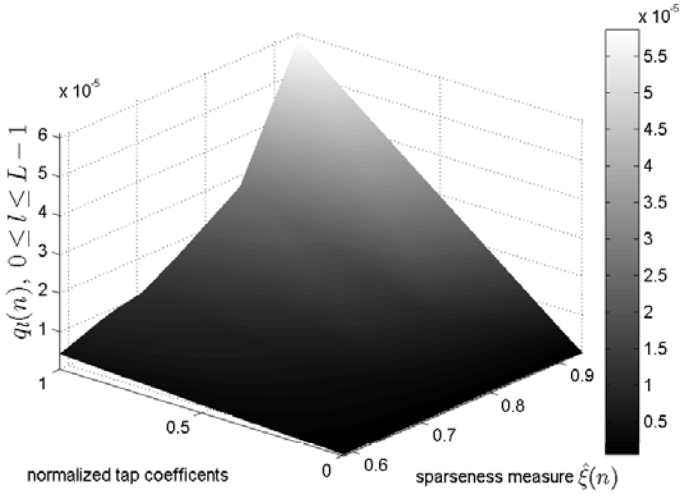

Fig. 8. Magnitude of $q_l(n)$ for $0 \le l \le L-1$ against the magnitude of coefficients $\widehat{h}_l(n)$ in SC-IPNLMS and different sparseness measures of 8 systems.

B. The SC-IPNLMS algorithm

We choose to incorporate sparseness-control into the IPNLMS algorithm (SC-IPNLMS) [16] in a different manner compared to SC-PNLMS and SC-MPNLMS because, as can be seen from (9), two terms are employed in IPNLMS for control of the mixture between proportionate and NLMS updates. The proposed SC-IPNLMS improves the performance of the IPNLMS by expressing $q_l(n)$ for $n \ge L$ as

$$q_l(n) = \left[\frac{1-0.5\widehat{\xi}(n)}{L}\right]\frac{(1-\alpha_{\mathrm{SC-IP}})}{2L} + \left[\frac{1+0.5\widehat{\xi}(n)}{L}\right]\frac{(1+\alpha_{\mathrm{SC-IP}})|\widehat{h}_l(n)|}{2\|\widehat{\mathbf{h}}(n)\|_1+\delta_{\mathrm{IP}}}. \quad (15)$$

As can be seen, for large $\widehat{\xi}(n)$ when the impulse response is sparse, the algorithm allocates more weight to the proportionate term of (9). For comparatively less sparse impulse responses, the algorithm aims to achieve the convergence of NLMS by applying a higher weighting to the NLMS term. An empirically chosen weighting of 0.5 in (15) is included to balance the performance between sparse and dispersive cases. In addition, normalization by L is introduced to reduce significant coefficient noise when the effective step-size is large for sparse AIRs with high $\widehat{\xi}(n)$.

Figure 8 illustrates the step-size control elements $q_l(n)$ for SC-IPNLMS in estimating different unknown AIRs. As can be seen, for dispersive AIRs, SC-IPNLMS allocates a uniform step-size across $h_l(n)$ while, for sparse AIRs, the algorithm distributes $q_l(n)$ proportionally to the magnitude of the coefficients. As a result of this distribution, the SC-IPNLMS algorithm varies the degree of NLMS and proportionate adaptations according to the nature of the AIRs. In contrast, in standard IPNLMS the mixing coefficient α_{IP} in (9) is fixed *a priori*. The SC-IPNLMS algorithm is described by (2)-(4), (12) and (15), as specified in Table I.

TABLE II
COMPLEXITY OF ALGORITHMS' COEFFICIENTS UPDATE - ADDITION (A), MULTIPLICATION (M), DIVISION (D), LOGARITHM (LOG) AND COMPARISON (C).

Algorithm	A	M	D	Log	C
NLMS	$L+3$	$L+3$	1	0	0
PNLMS	$2L+1$	$5L+2$	2	0	$2L$
SC-PNLMS	$4L+2$	$6L+4$	3	0	$2L$
IPNLMS	$3L+2$	$5L+2$	2	0	0
SC-IPNLMS	$4L+5$	$6L+8$	3	0	0
MPNLMS	$3L+1$	$6L+2$	2	L	$2L$
SC-MPNLMS	$5L+2$	$7L+4$	3	L	$2L$

V. COMPUTATIONAL COMPLEXITY

The relative complexity of NLMS, PNLMS, SC-PNLMS, IPNLMS, SC-IPNLMS, MPNLMS and SC-MPNLMS in terms of the total number of additions (A), multiplications (M), division (D), logarithm (Log) and comparisons (C) per iteration for adaptation of filter coefficients is assessed in Table II. The additional complexity of the proposed sparseness-controlled algorithms, on top of their conventional method, arises from the computation of the sparseness measure $\widehat{\xi}(n)$. Given that $L/(L-\sqrt{L})$ in (10) can be computed off-line, the remaining l-norms require an additional $2L$ additions and L multiplications. The SC-PNLMS and SC-MPNLMS algorithms additionally require computations for (14). Alternatively, a look-up table with values of $\rho(n)$ defined in (14) can be computed for $0 \le \widehat{\xi}(n) \le 1$. Segment PNLMS (SPNLMS) is proposed in [27], to approximate the μ-law function in MPNLMS using line segments. Since $\|\widehat{\mathbf{h}}(n)\|_1$ computation is already available from IPNLMS in (9), SC-IPNLMS only requires an additional $L+3$ additions, $L+6$ multiplications and 1 division. As we shall see, the increase in the complexity is compromised by the algorithm's performance. Consequently, the trade-off between complexity and performance depend on the design choice for a particular application.

VI. SIMULATION RESULTS

We present simulation results to evaluate the performance of the proposed SC-PNLMS, SC-MPNLMS and SC-IPNLMS algorithms in the context of AEC. In addition, we show an example case of how SC-IPNLMS can be employed in NEC. Throughout our simulations, algorithms were tested using a zero mean WGN and a male speech signal as inputs while another WGN sequence $w(n)$ was added to give an SNR of 20 dB. We assumed that the length of the adaptive filter $L = 1024$ is equivalent to that of the unknown system. Two receiving room impulse responses $\mathbf{h}(n)$ for AEC simulations have been used as described in Fig. 3. The sparseness measure of these AIRs are computed using (10) giving (a) $\xi(n) = 0.83$ and (b) $\xi(n) = 0.59$ respectively.

A. Effect of λ on the performance of SC-PNLMS for AEC

SC-PNLMS was tested as shown in Fig. 9 for different λ values in (14) to illustrate the time taken to reach -20 dB

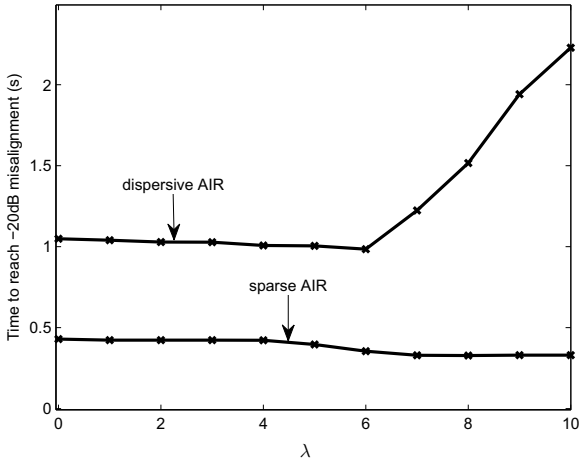

Fig. 9. Time to reach -20 dB normalized misalignment level for different values of λ in SC-PNLMS using WGN input signal. Impulse response in Fig. 3 (a) and (b) used as sparse AIR and dispersive AIR respectively. [$\mu_{\mathrm{SC-PNLMS}} = 0.3$, SNR $= 20$ dB]

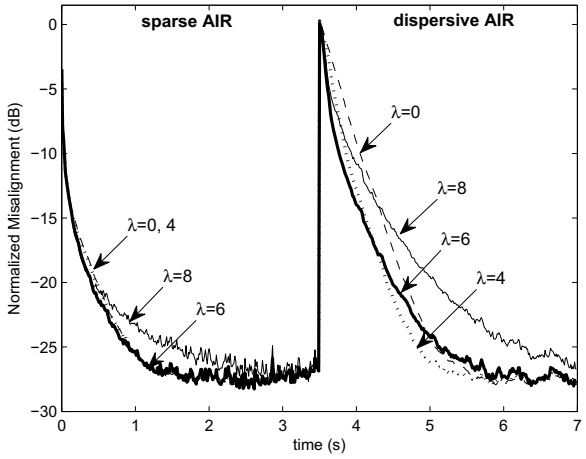

Fig. 10. Convergence of the SC-PNLMS for different values of λ using WGN input signal with an echo path change at 3.5 s. Impulse response is changed from Fig. 3 (a) to (b) and $\mu_{\mathrm{SC-PNLMS}} = 0.3$, SNR $= 20$ dB.

normalized misalignment using a WGN sequence as the input signal. A step-size of $\mu = 0.3$ was used in this experiment. We see from the result that, for each case of λ, the SC-PNLMS has a higher rate of convergence for a sparse system compared to a dispersive system. This is due to the initialization choice of $\widehat{\mathbf{h}}(0) = \mathbf{0}_{L\times 1}$, where most filter coefficients are initialized close to their optimal values. In addition, a smaller value of λ is favorable for the dispersive AIR, since SC-PNLMS performs similarly to NLMS for small λ values. On the contrary, a higher value for λ is desirable for the sparse case. It can be noted that SC-PNLMS is exactly NLMS for $\lambda = 0$. It can also be seen that a range of good value for λ is $4 \leq \lambda \leq 6$. Figure 10 shows the performance of SC-PNLMS with an echo path change introduced from Fig. 3 (a) to (b) at 4.5 s, for $\lambda = 0, 4, 6$ and 8. We observe from this result that the convergence rate of SC-PNLMS is high when λ is small for a dispersive channel. This is because, as explained in Section IV-A, the proposed algorithm inherits properties of the NLMS for a small λ value. For a high λ, the SC-PNLMS algorithm inherits properties of PNLMS giving good performance for sparse AIR before the echo path change. As can be seen, a good compromise of λ is given by $\lambda = 6$.

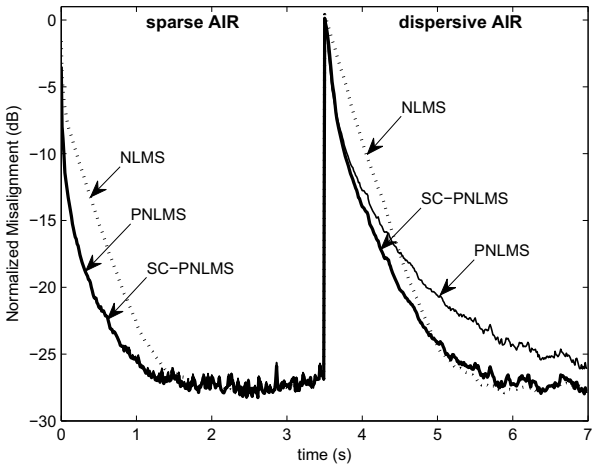

Fig. 11. Relative convergence of NLMS, PNLMS and SC-PNLMS using WGN input signal with an echo path change at 3.5 s. Impulse response is changed from that shown from Fig. 3 (a) to (b) and $\mu_{\mathrm{NLMS}} = \mu_{\mathrm{PNLMS}} = \mu_{\mathrm{SC-PNLMS}} = 0.3$, SNR $= 20$ dB.

B. Convergence performance of SC-PNLMS for AEC

Figure 11 compares the performance of NLMS, PNLMS and SC-PNLMS using WGN as the input signal. The step-size parameter for each algorithm is chosen such that all algorithms achieve the same steady-state. This is achieved by setting $\mu_{\mathrm{NLMS}} = \mu_{\mathrm{PNLMS}} = \mu_{\mathrm{SC-PNLMS}} = 0.3$. An echo path change was introduced from Fig. 3(a) to 3(b) while λ for the SC-PNLMS algorithm is set to 6. It can be seen from Fig. 11 that the convergence rate of SC-PNLMS is as fast as PNLMS for sparse and much better than PNLMS for dispersive, therefore achieving our objective of improving robustness to varying sparseness. This is because SC-PNLMS inherits the beneficial properties of both PNLMS and NLMS. It can be seen from the result that SC-PNLMS achieves high rate of convergence similar to PNLMS giving approximately 5 dB improvement in normalized misalignment during initial convergence compared to NLMS for a sparse AIR. After the echo path change, for a dispersive AIR, the SC-PNLMS maintains its high convergence rate over NLMS and PNLMS giving approximately 4 dB improvement in normalized misalignment compared to PNLMS.

Figure 12 shows simulation results for a male speech input signal where we used the same parameters as in the case of WGN input signal. As can be seen, the proposed SC-PNLMS algorithm achieves the highest rate of convergence, giving convergence as fast as PNLMS and approximately 7 dB improvement during initial convergence compared to NLMS for the sparse AIR. For dispersive AIR, SC-PNLMS performs almost the same as NLMS with approximately 4 dB improvement compared to PNLMS.

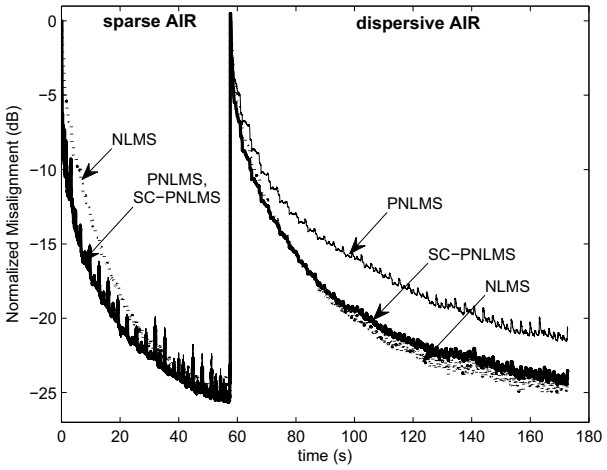

Fig. 12. Relative convergence of NLMS, PNLMS and SC-PNLMS using speech input signal with echo path changes at 58 s. Impulse response is changed from that shown in Fig. 3 (a) to (b) and μ_{NLMS} = 0.3, μ_{PNLMS} = $\mu_{\mathrm{SC-PNLMS}}$ = 0.1, SNR = 20 dB.

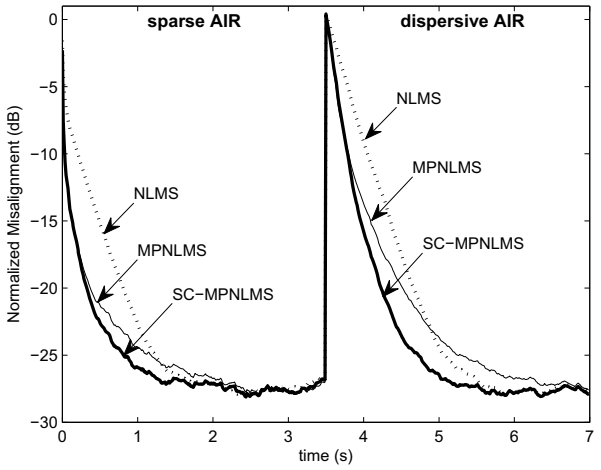

Fig. 13. Relative convergence of NLMS, MPNLMS and SC-MPNLMS using WGN input signal with an echo path change at 3.5 s. Impulse response is changed from that shown from Fig. 3 (a) to (b) and μ_{NLMS} = 0.3, μ_{MPNLMS} = $\mu_{\mathrm{SC-MPNLMS}}$ = 0.25, SNR = 20 dB.

C. Convergence performance of SC-MPNLMS for AEC

Figure 13 illustrates the performance of NLMS, MPNLMS and SC-MPNLMS using WGN as the input signal. As before, the step-sizes were adjusted to achieve the same steady-state misalignment for all algorithms. This corresponds to $\mu_{\mathrm{NLMS}} = 0.3$, $\mu_{\mathrm{MPNLMS}} = \mu_{\mathrm{SC-MPNLMS}} = 0.25$. We have also used $\lambda = 6$ for SC-MPNLMS. As can be seen from this result, the SC-MPNLMS algorithm attains approximately 8 dB improvement in normalized misalignment during initial convergence compared to NLMS and same initial performance followed by approximately 2 dB improvement over MPNLMS for the sparse AIR. After the echo path change, SC-MPNLMS achieves approximately 3 dB improvement compared to MPNLMS and about 8 dB better performance than NLMS for dispersive AIR. As shown in Fig. 14, with speech signal as the input, the proposed SC-MPNLMS algorithm achieves approximately 10 dB improvement during initial convergence compared to NLMS and 2 dB compared to MPNLMS for the sparse AIR. For dispersive AIR, the SC-MPNLMS algorithm achieves an improvement of approximately 4 dB compared to both NLMS and MPNLMS. It is also noted that NLMS achieves approximately 7 dB better steady-state performance than the MPNLMS-based approaches for this example with speech input. This is attributed in [4] to sensitivity to eigenvalue spread of the speech signal's autocorrelation matrix.

D. Convergence performance of SC-IPNLMS for AEC

For SC-IPNLMS performance comparison, we used $\mu_{\mathrm{NLMS}} = \mu_{\mathrm{IPNLMS}} = 0.3$, $\mu_{\mathrm{SC-IPNLMS}} = 0.7$ in order to attain same steady state performance. Proportionality control factors $\alpha_{\mathrm{IP}} = \alpha_{\mathrm{SC-IP}} = -0.75$ have been used for both IPNLMS and SC-IPNLMS. It can be seen from Fig. 15 and 16 that by using both WGN and speech input signals, SC-IPNLMS achieves approximately 10 dB improvement in normalized misalignment during initial convergence compared

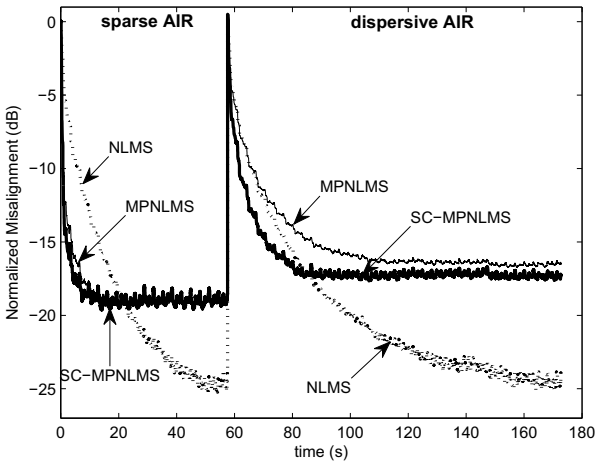

Fig. 14. Relative convergence of NLMS, MPNLMS and SC-MPNLMS using speech input signal with echo path changes at 58 s. Impulse response is changed from that shown in Fig. 3 (a) to (b) and μ_{NLMS} = 0.3, μ_{MPNLMS} = $\mu_{\mathrm{SC-MPNLMS}}$ = 0.25, SNR = 20 dB.

to NLMS for the sparse AIR. For a dispersive AIR, the SC-IPNLMS achieves a 5 dB improvement compared to NLMS. For a speech input, the improvement of SC-IPNLMS over IPNLMS is 3 dB for both sparse and dispersive AIRs. On the other hand, the improvement of SC-IPNLMS compared to NLMS are 10 dB and 6 dB for sparse and dispersive AIRs, respectively.

E. Convergence performance of the algorithms for various AIRs with different sparseness in AEC

We extracted eight different impulse responses from the set of AIRs with sparseness measure $0.58 \leq \xi \leq 0.93$ as shown in Fig. 4. The time taken to reach -20 dB normalized misalignment is plotted against $\xi(n)$ for NLMS, PNLMS, SC-PNLMS, IPNLMS and SC-IPNLMS in Fig. 17, and for NLMS, MPNLMS and SC-MPNLMS in Fig. 18. As before, all step-sizes have been adjusted so that the algorithms achieve the

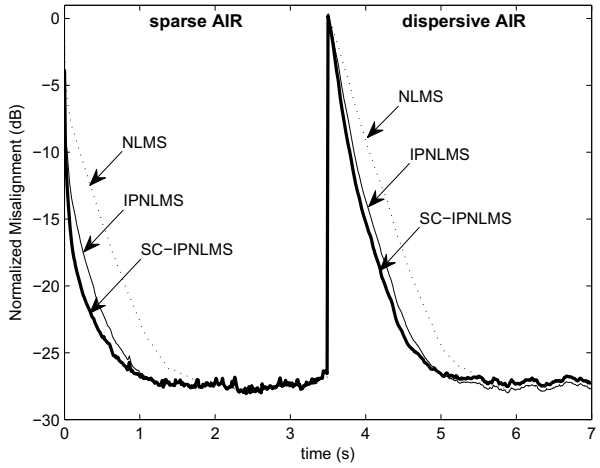

Fig. 15. Relative convergence of NLMS, IPNLMS and SC-IPNLMS using WGN input signal with an echo path change at 3.5 s. Impulse response is changed from that shown from Fig. 3 (a) to (b) and μ_{NLMS} = μ_{IPNLMS} = 0.3, $\mu_{\mathrm{SC-IPNLMS}}$ = 0.7, SNR = 20 dB.

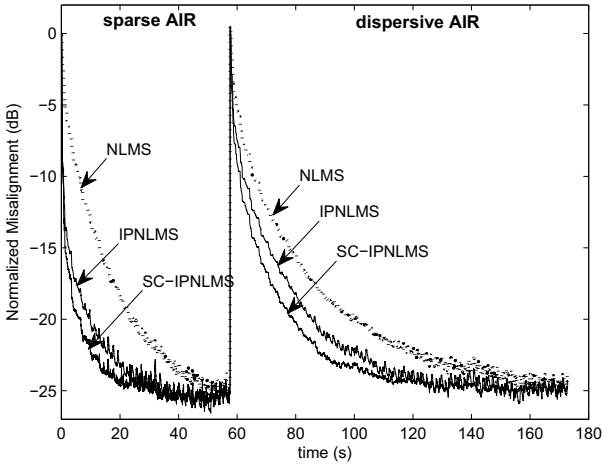

Fig. 16. Relative convergence of NLMS, IPNLMS and SC-IPNLMS using speech input signal with echo path changes at 58 s. Impulse response is changed from that shown in Fig. 3 (a) to (b) and μ_{NLMS} = μ_{IPNLMS} = 0.3, $\mu_{\mathrm{SC-IPNLMS}}$ = 0.8, SNR = 20 dB.

same steady-state normalized misalignment. These correspond to $\mu_{\mathrm{NLMS}} = \mu_{\mathrm{PNLMS}} = \mu_{\mathrm{SC-PNLMS}} = \mu_{\mathrm{IPNLMS}} = 0.3$, $\mu_{\mathrm{MPNLMS}} = \mu_{\mathrm{SC-MPNLMS}} = 0.25$ and $\mu_{\mathrm{SC-IPNLMS}} = 0.7$. A zero mean WGN was used as an input signal while another WGN sequence w(n) was added to achieve an SNR of 20 dB. It can be seen that when the AIRs are sparse, the speed of initial convergence increases significantly for each algorithm. This is because many of the filter coefficients are initialized close to their optimum values since during initialization, $\widehat{\mathbf{h}}(0) = \mathbf{0}_{L\times 1}$. In addition, the sparseness-controlled algorithms (SC-PNLMS, SC-MPNLMS and SC-IPNLMS) give the overall best performance compare to their conventional methods across the range of sparseness measure. This is because the proposed algorithms take into account the sparseness measure of the estimated impulse response at each iteration.

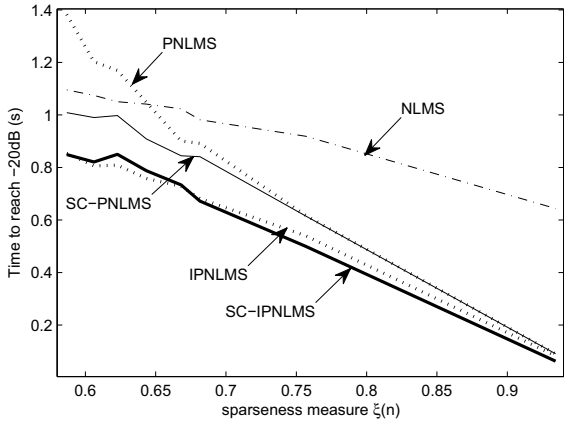

Fig. 17. Time to reach the -20dB normalized misalignment against different sparseness measures of 8 systems for NLMS, PNLMS, SC-PNLMS, IPNLMS and SC-IPNLMS.

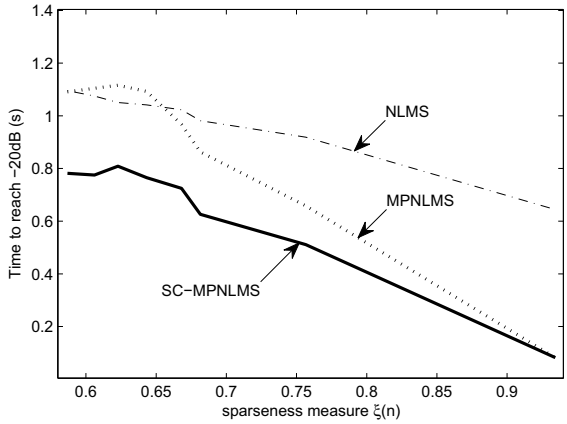

Fig. 18. Time to reach the -20dB normalized misalignment against different sparseness measures of 8 systems for NLMS, MPNLMS and SC-MPNLMS.

F. Convergence performance of SC-IPNLMS for NEC

We provide additional simulations to illustrate the performance of SC-IPNLMS in the context of sparse adaptive NEC, such as may occur in network gateways for mixed packet-switched and circuit-switched networks. Figure 19 shows two impulse responses, sampled at 8 kHz comprising a 12 ms active region located within a total duration of 128 ms. The sparseness of these impulse responses computed using (12) are (a) $\xi(n) = 0.88$ and (b) $\xi(n) = 0.85$ respectively. As before, we used a WGN input signal while another WGN sequence is added to give an SNR of 20 dB. Figure 20 shows the performances of NLMS, IPNLMS, for $\alpha_{\mathrm{IP}} = -0.5$ and -0.75, and the proposed SC-IPNLMS algorithm with $\alpha_{\mathrm{SC-IP}} = -0.75$. An echo path change was introduced using impulse responses as shown from Fig. 19 (a) to (b) at 3.5 s. We can see from the result that the performance of IPNLMS is dependent on α_{IP}. More importantly, a faster rate of convergence can be seen for SC-IPNLMS compared to NLMS and IPNLMS both at initial convergence and also after the echo path change.

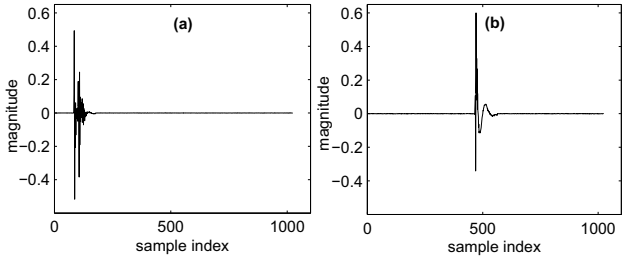

Fig. 19. Sparse impulse responses, sampled at 8 kHz, giving (a) $\xi(n) = 0.88$ and (b) $\xi(n) = 0.85$ respectively.

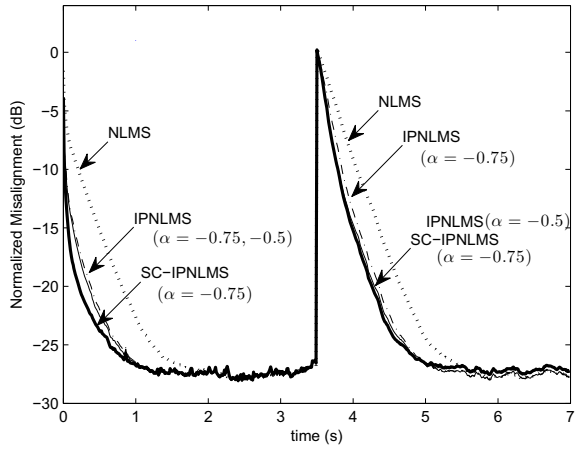

Fig. 20. Relative convergence of NLMS, IPNLMS for $\alpha = -0.5$ and -0.75 and SC-IPNLMS using WGN input signal with an echo path change at 3.5 s. Impulse response is changed from that shown in Fig. 19 (a) to (b) and μ_{NLMS} = μ_{IPNLMS} = 0.3, $\mu_{\mathrm{SC-IPNLMS}}$ = 0.7, SNR = 20 dB.

VII. Conclusion

We have presented a class of sparseness-controlled algorithms which achieves improved convergence compared to classical NLMS and typical sparse adaptive filtering algorithms. We have incorporated the sparseness measure into PNLMS, MPNLMS and IPNLMS for AEC to achieve fast convergence that is robust to the level of sparseness encountered in the impulse response of the echo path. The resulting SC-PNLMS, SC-MPNLMS and SC-IPNLMS algorithms take into account the sparseness measure via a modified coefficient update function.

It has been shown that the proposed sparseness-controlled algorithms are robust to variations in the level of sparseness in AIR with only a modest increase in computational complexity. Moreover, we have shown that these proposed algorithms have same or faster convergence in NEC.

References

[1] J. Radecki, Z. Zilic, and K. Radecka, "Echo cancellation in IP networks," in *Proc. Fourty-Fifth Midwest Symposium on Circuits and Systems*, vol. 2, 2002, pp. 219–222.

[2] D. L. Duttweiler, "Proportionate normalized least mean square adaptation in echo cancellers," *IEEE Trans. Speech Audio Processing*, vol. 8, no. 5, pp. 508–518, Sep. 2000.

[3] A. W. H. Khong, J. Benesty, and P. A. Naylor, "Stereophonic acoustic echo cancellation: Analysis of the misalignment in the frequency domain," *IEEE Signal Processing Lett.*, vol. 13, pp. 33–36, 2006.

[4] H. Deng and M. Doroslovacki, "Wavelet-based MPNLMS Adaptive Algorithm for Network Echo Cancellation," *EURASIP Journal on Audio, Speech, and Music Processing*, 2007.

[5] R. H. Kwong and E. Johston, "A variable step-size algorithm for adaptive filtering," *IEEE Trans. Signal processing*, vol. 40, pp. 1633–1642, 1992.

[6] C. Rusu and F. N. Cowan, "The convex variable step size (CVSS) algorithm," *IEEE Signal processing Letter*, vol. 7, pp. 256–258, 2000.

[7] J. Sanubari, "A new variable step size method for the LMS adaptive filter," in *IEEE Asia-Pacific Conference on Circuits and systems*, 2004.

[8] B. A. Schnaufer and W. K. Jenkins, "New data-reusing lms algorithms for improved convergence," in *in Proc. Twenty-Seventh Asilomar Conf. Signals, Syst., Comput.*, 1993.

[9] K. A. G. Robert A. Soni and W. K. Jenkins, "Low-complexity data reusing methods in adaptive filtering," *IEEE Transactions on signal processing*, vol. 52, no. 2, pp. 394–405, Feb 2004.

[10] A. W. H. Khong and P. A. Naylor, "Selective-tap adaptive algorithms in the solution of the non-uniqueness problem for stereophonic acoustic echo cancellation," *IEEE Signal Processing Lett.*, vol. 12, no. 4, pp. 269–272, Apr. 2005.

[11] P. A. Naylor and A. W. H. Khong, "Affine projection and recursive least squares adaptive filters employing partial updates," in *Proc. Thirty-Eighth Asilomar Conference on Signals, Systems and Computers*, vol. 1, Nov. 2004, pp. 950–954.

[12] K. A. Lee and S. Gan, "Improving convergence of the NLMS algorithm using constrained subbands updates," *IEEE Signal Processing Lett.*, vol. 11, no. 9, pp. 736–739, Sept. 2004.

[13] A. Deshpande and S. L. Grant, "A new multi-algorithm approach to sparse system adaptation," in *Proc. European Signal Process. Conf.*, 2005.

[14] S. L. Gay, "An efficent, fast converging adaptive filter for network echo cancellation," vol. 1, November 1998, pp. 394–398.

[15] J. Benesty and S. L. Gay, "An improved PNLMS algorithm," in *Proc. IEEE Int. Conf. Acoustics Speech Signal Processing*, vol. 2, 2002, pp. 1881–1884.

[16] A. W. H. Khong and P. A. Naylor, "Efficient use of sparse adaptive filters," in *Signals, Systems and Computers, 2006. ACSSC '06. Fortieth Asilomar Conference*, Oct 2006.

[17] M. A. Mehran Nekuii, "A fast converging algorithm for network echo cancelation," *IEEE Signal Processing Letter*, vol. 11, pp. 427–430, 2004.

[18] H. Deng and M. Doroslovacki, "Improving convergence of the PNLMS algorithm for sparse impulse response identification," *IEEE Signal Processing Lett.*, vol. 12, no. 3, pp. 181–184, Mar. 2005.

[19] E. Hänsler, "The hands-free telephone problem- an annotated bibliography," *Signal Processing*, vol. 27, no. 3, pp. 259–271, Jun. 1992.

[20] R. Ahmad, A. W. Khong, and P. A. Naylor, "Proportionate frequency domain adaptive algorithms for blind channel identification," in *Proc. IEEE Int. Conf. Acoustics Speech Signal Processing*, vol. 5, May 2006, pp. V29–V32.

[21] G. W. Elko, E. Diethorn, and T. Gänsler, "Room impulse response variation due to thermal fluctuation and its impact on acoustic echo cancellation," in *Proc. Int. Workshop on Acoustic Echo and Noise Control*, 2003, pp. 67–70.

[22] H. Sabine, "Room acoustics," *Transactions of the IRE Professional Group on Room Acoustics*, vol. 1, no. 4, pp. 4–12, Jul. 1953.

[23] J. Benesty, Y. A. Huang, J. Chen, and P. A. Naylor, "Adaptive algorithms for the identification of sparse impulse responses," in *Selected methods for acoustic echo and noise control*, E. Hänsler and G. Schmidt, Eds. Springer, 2006, ch. 5, pp. 125–153.

[24] J. B. Allen and D. A. Berkley, "Image method for efficiently simulating small-room acoustics," *J. Acoust. Soc. Amer.*, vol. 65, no. 4, pp. 943–950, Apr. 1979.

[25] P. M. Peterson, "Simulating the response of multiple microphones to a single acoustic source in a reverberant room." vol. 80, no. 5, pp. 1527–1529, Nov 1986.

[26] K. Wagner and M. Doroslovacki, "Towards Analytical Convergence Analtsis of Proportion-type NLMS Algorithms," in *Proc. IEEE Int. Conf. Acoustics Speech Signal Processing*, 2008, pp. 3825–3828.

[27] H. Deng and M. Doroslovacki, "Proportionate adaptive algorithms for network echo cancellation," *IEEE Transactions on Signal Processing*, vol. 54, no. 5, pp. 1794–1803, May 2006.